doi:10.1017/S1431927618007833
Microsc. Microanal. 24 (Suppl 1), 2018

Electron holography study on vortex beam phases in real space

K. Harada[1], K. Shimada[1], Y. A. Ono[1], Y. Iwasaki[1], K. Niitsu[1,#], and D. Shindo[1,2]

[1.] CEMS, RIKEN, Hatoyama, Saitama 350-0395, Japan.
[2.] IMRAM, Tohoku Univ., Sendai, Miyagi 980-8577, Japan.

Recently electron-microscope studies on vortex beams (VBs) have covered not only physical properties as a new electron probe [1,2] but also applications to materials[3]. For practical applications of VBs, direct measurements of phase distributions of the VBs are important. In the present study, we used electron interferometry in two waves, the first-order diffraction wave and the zeroth-order plane wave, to record phase distributions of VBs as holograms [2]. The principle of this experiment is the same as that of Gabor's original in-line holography.

Figure 1 shows an optical system for recording interferograms as holograms of VBs, and insets are micrographs and interferograms at each position in the optical system. The upper inset shows fork-shaped gratings and the second upper inset shows the hologram under the under-focus condition. The third inset shows diffraction from the grating with the zeroth-order centered diffraction spot and the first- and second-order diffraction spots, which are all ring-shaped. The bottom inset shows the hologram under the over-focus condition. In the following, the right-hand side diffraction beams (VBs) are defined as direct waves and the left-hand side diffraction beams (VBs), conjugate waves. In Fig. 2 the upper row shows illustrations of the interference relation between wavefronts, VBs and reference waves, and the lower row shows simulation results of interference fringes. These simple and vortex-shaped fringes were formed by two-wave interference.

Since these holograms (insets in Fig.1) are recorded in principle through two-wave interferometry, the conventional reconstruction procedure, i.e., the Fourier transform method, can be utilized. Figures 3 shows reconstructed amplitude images ((a), (c) and (e)) and phase images ((b), (d) and (f)) under the under-focus condition. In this numerical reconstruction, compensation for defocusing distance from the fork-shaped grating to the recorded plane can also be carried out. The numerical compensation was determined for the conjugate waves in (a) and (b), and compensation for the reversed parameters was also determined for direct waves in (e) and (f) in the same way. The amplitude distribution of the conjugate wave (left-hand side) in (a) shows a uniform structure and the phase distribution of the conjugate wave in (b) shows helical and plane structures, indicating the VB in real space. Similar features are shown in Figs. 3(e) and (f), even though numerical calculation parameters are reversed from those of the conjugate waves.

In conclusion, the amplitude and phase distributions of VBs in real space were successfully reconstructed through electron holography. We believe that this method for analyzing VBs, especially for analyzing phase distributions, will be effective in practical applications of VBs.

References:
[1] B. J. McMorran, *et al.*, *Phyl. Trans. R. Soc. A* **375** (2017) 20150434.
[2] K. Harada *et al.*, *Microsc. Microanal.* **23** (2017) 588; ibid. **21** (2015) 699; ibid. **20** (2014) 274.

[3] V. Grillo *et al.*, *Nature Comm.* **8** (2017) 689.
[4] # present address: Materials Science & Engineering, Kyoto University, Kyoto 606-8501, Japan.

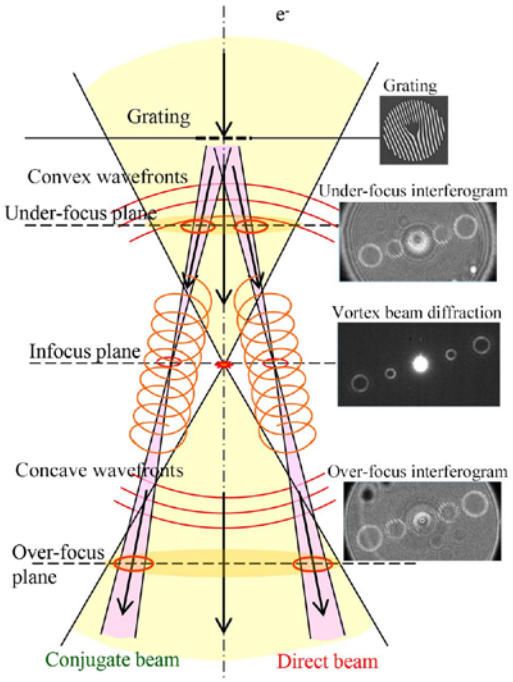

Figure 1. Schematic diagram of optical system.

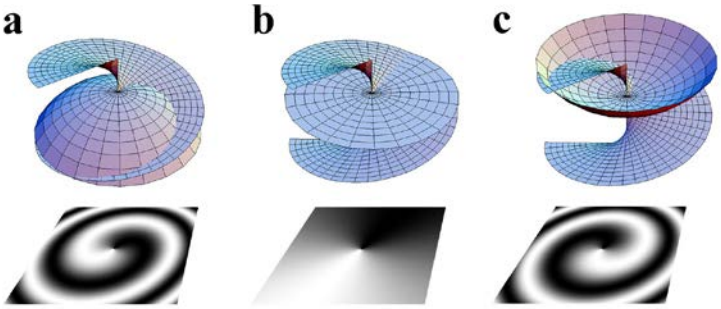

Figure 2. Illustration of wavefronts of helical wave (VBs) and reference waves in the upper row, and schematics of interference relations in the lower row. (a) VB with convex wavefront under the under-focus condition, (b) VB with plane wavefront inunder the infous condition, and (c) VB with concave wavefront under the over-focus condition.

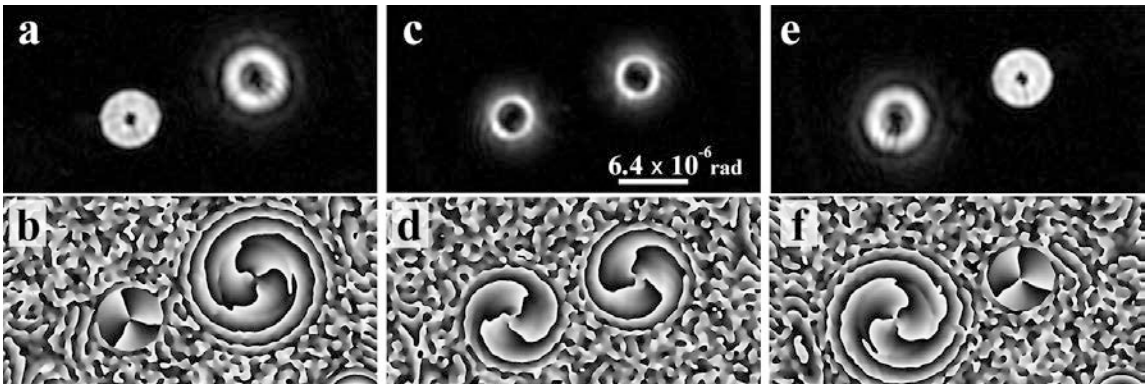

Figure 3. Reconstructed amplitude and phase images of the first-order VBs from the under-focused interferogram; (a) amplitude image of the conjugate VB after compensation of defocus distance, (b) phase image of the conjugate VB after compensation of defocus distance, (c) and (d) amplitude and phase image without compensation of defocusing, (e) and (f) amplitude and phase images of the direct VB after compensation of defocus distance.

https://doi.org/10.1017/S1431927618007833 Published online by Cambridge University Press